

Anion Separation by Selective Crystallization of Metal–Organic Frameworks

Radu Custelcean,* Tamara J. Haverlock, and Bruce A. Moyer

Chemical Sciences Division, Oak Ridge National Laboratory, Oak Ridge, Tennessee 37831-6119

Received May 31, 2006

A novel approach for the separation of anions from aqueous mixtures was demonstrated, which involves their selective crystallization with metal–organic frameworks (MOFs) containing urea functional groups. Self-assembly of Zn^{2+} with the *N,N'*-bis(*m*-pyridyl)urea (BPU) linker results in the formation of one-dimensional MOFs including various anions for charge balance, which interact to different extents with the zinc nodes and the urea hydrogen-bonding groups, depending on their coordinating abilities. Thus, Cl^- , Br^- , I^- , and SO_4^{2-} , in the presence of BPU and Zn^{2+} , form MOFs from water, in which the anions coordinate the zinc and are hydrogen-bonded to the urea groups, whereas NO_3^- and ClO_4^- anions either do not form MOFs or form water-soluble discrete coordination complexes under the same conditions. X-ray diffraction, FTIR, and elemental analysis of the coordination polymers precipitated from aqueous mixtures containing equivalent amounts of these anions indicated total exclusion of the oxoanions and selective crystallization of the halides in the form of solid solutions with the general composition $ZnCl_xBr_yI_z \cdot BPU$ ($x + y + z = 2$), with an anti-Hofmeister selectivity. The concomitant inclusion of the halides in the same structural frameworks facilitates the rationalization of the observed selectivity on the basis of the diminishing interactions with the zinc and urea acidic centers in the MOFs when going from Cl^- to I^- , which correlates with decreasing anionic charge density in the same order. The overall crystal packing efficiency of the coordination frameworks, which ultimately determines their solubility, also plays an important role in the anion crystallization selectivity under thermodynamic equilibration.

Introduction

Research in the area of metal–organic frameworks (MOFs), or coordination polymers, crystalline materials self-assembled from transition metal cations and organic coordinating linkers, has witnessed a spectacular growth in the past decade.¹ Whereas the initial focus was on synthesis and structural aspects, more recently, the attention has shifted to possible applications of these materials, preponderantly in gas storage,² catalysis,³ and chemical separations.⁴ When neutral linkers are employed, the resulting MOFs are cationic and thus intrinsically include charge-balancing anions, which

inspired the use of such networks for anion exchange, similarly to ion-exchange resins.⁵ Given the pervasiveness of separations in the chemical industry,⁶ the potential impact of MOFs as a vehicle for novel separations is considerable, yet the potential of this class of materials in this regard is

* To whom correspondence should be addressed. E-mail: custelcean@ornl.gov.

(1) (a) Ockwig, N. W.; Delgado-Friedrichs, O.; O'Keeffe, M.; Yaghi, O. M. *Acc. Chem. Res.* **2005**, *38*, 176. (b) Férey, G.; Mellot-Draznieks, C.; Serre, C.; Millange, F. *Acc. Chem. Res.* **2005**, *38*, 217. (c) Fletcher, A. J.; Thomas, K. M.; Rosseinsky, M. J. *J. Solid State Chem.* **2005**, *178*, 2491. (d) Kitagawa, S.; Kitaura, R.; Noro, S. *Angew. Chem., Int. Ed.* **2004**, *43*, 2334. (e) Janiak, C. *Dalton Trans.* **2003**, 2781. (f) James, S. L. *Chem. Soc. Rev.* **2003**, *32*, 276. (g) Moulton, B.; Zaworotko, M. J. *Chem. Rev.* **2001**, *101*, 1629. (h) Hoskins, B. F.; Robson, R. *J. Am. Chem. Soc.* **1990**, *112*, 1546.

(2) (a) Rowsell, J. L. C.; Yaghi, O. M. *Angew. Chem., Int. Ed.* **2005**, *44*, 4670. (b) Bourrelly, S.; Llewellyn, P. L.; Serre, C.; Millange, F.; Loiseau, T.; Férey, G. *J. Am. Chem. Soc.* **2005**, *127*, 13519. (c) Matsuda, R.; Kitaura, R.; Kitagawa, S.; Kubota, Y.; Belosludov, R. V.; Kobayashi, T. C.; Sakamoto, H.; Chiba, T.; Takata, M.; Kawazoe, Y.; Mita, Y. *Nature* **2005**, *238*, 1308. (d) Millward, A. R.; Yaghi, O. M. *J. Am. Chem. Soc.* **2005**, *127*, 17998. (e) Kaye, S. S.; Long, J. R. *J. Am. Chem. Soc.* **2005**, *127*, 6506. (f) Chun, H.; Dybtsev, D. N.; Kim, H.; Kim, K. *Chem.—Eur. J.* **2005**, *11*, 3521. (g) Kesaneli, B.; Cui, Y.; Smith, M. R.; Bittner, E. W.; Bockrath, B. C.; Lin, W. *Angew. Chem., Int. Ed.* **2005**, *44*, 72. (h) Zhao, X. B.; Xiao, B.; Fletcher, A. J.; Thomas, K. M.; Bradshaw, D.; Rosseinsky, M. J. *Science* **2004**, *306*, 1012. (i) Pan, L.; Sander, M. B.; Huang, X. Y.; Li, J.; Smith, M.; Bittner, E.; Bockrath, B.; Johnson, J. K. *J. Am. Chem. Soc.* **2004**, *126*, 1308.

(3) (a) Fujita, M.; Kwon, Y. J.; Washizu, S.; Okura, K. *J. Am. Chem. Soc.* **1994**, *116*, 1151. (b) Wu, C.-D.; Hu, A.; Zhang, L.; Lin, W. *J. Am. Chem. Soc.* **2005**, *127*, 8940. (c) Dybtsev, D. N.; Nuzhdin, A. L.; Chun, H.; Bryliakov, K. P.; Talsi, E. P.; Fedin, V. P.; Kim, K. *Angew. Chem., Int. Ed.* **2006**, *45*, 916.

only beginning to be explored. Results have so far focused on adsorption⁴ and ion exchange⁵ processes, applications in which MOFs are treated as the separations agents. Surprisingly, the crystallization process involved in the synthesis of MOFs has not in itself been explored as a tool for separations, though precipitation or crystallization is one of the most important techniques for the recovery of species from solution.

The anion-exchange process in MOFs has generally been assumed to occur by a solid-state mechanism via diffusion of the anions in and out of the framework as opposed to disintegration and reassembly of the crystals. Such an assumption is generally based on the low solubility of MOFs in most solvents and, in some cases, on the structural similarities of the initial and final frameworks. However, a recent study found that, at least in certain one-dimensional coordination polymers, the apparent anion exchange from water is more likely solvent-mediated, involving dissolution of the initial framework and recrystallization of the final one.⁷ Thus, it seems to us that the problem of anion separation using MOFs may be more effectively approached as one of selective crystallization. Such an approach avoids the often-encountered problem of slow ion-exchange kinetics in the solid state and broadens the applicability of MOFs to one of the most commercially important separation technologies.

Regardless of the operating mechanism, MOFs may offer unique opportunities for anion separation, particularly in terms of selectivity. Unlike the resin counterparts, MOFs have well-defined crystalline structures, and therefore, different factors such as the anion size, shape, or packing inside the crystal may control the anion inclusion.⁸ Under these circumstances, certain anions can be totally excluded from the framework if they lack the proper size and symmetry, which can lead to unparalleled selectivities. Another advantage over polymeric resins is that the crystallinity of MOFs allows for detailed structural characterization by X-ray diffraction methods, which can facilitate their rational design and simplify interpretation of the observed separation properties. Toward this end, it is important within the exchange paradigm to find systems that preserve a common structural framework upon anion exchange, to allow for unambiguous

formulations of structure-selectivities relationships. Unfortunately, this stringent requirement has rarely been met so far, which limits our current understanding of the factors governing anion selectivity in MOFs. Moreover, because competition experiments or anion-exchange isotherms have not been reported, it is difficult to assess the anion selectivity of MOFs studied to date. Pairwise anion-exchange experiments in a silver-polynitrile coordination network reported recently provided an indication of the anion binding affinity in this class of materials, which was found to decrease in the order $\text{ClO}_4^- > \text{NO}_3^- > \text{CF}_3\text{SO}_3^- > \text{Cl}^-$, coinciding with the Hofmeister bias favoring the less hydrated, less hydrophilic anions.^{5b} Such a behavior is similar with classical anion exchange processes found in solvent extraction or resin ion exchange, which are mainly governed by anion-solvation phenomena.⁹ Accordingly, anions with higher charge density are more strongly hydrated and therefore more difficult to transfer into the more weakly solvating or interacting medium usually found in an organic solvent, resin, or coordination polymer. The Hofmeister bias can, however, be attenuated or even reversed when anion receptors containing strong hydrogen-bonding groups¹⁰ or Lewis acid centers¹¹ are employed, as they effectively replace the hydration shell of the extracted anions.

By analogy with the discrete anion receptors in solution, we reasoned that functionalization of MOFs with hydrogen-bonding groups acting as specific coordination sites for the included anion could significantly enhance the solid-state anion selectivity in this class of materials. Furthermore, the transition metal nodes in MOFs may act as Lewis acid coordination sites for the anions and thus work in concert with the hydrogen-bonding groups to overcome the Hofmeister bias. Among the myriad of hydrogen-bonding groups utilized for anion binding, urea stands out as particularly attractive, as it is capable of chelating the targeted anion with its two preorganized NH protons, thus offering enhanced binding strength and recognition abilities.¹² Along this line, we recently designed a tris-urea linker derived from tren, which self-assembled with Ag^+ into a MOF that exclusively encapsulated sulfate anions through the unprecedented formation of 12 complementary hydrogen bonds from six urea groups.¹³ This material, however, proved ineffective for anion exchange, as other anions with lower charge density than sulfate could not compete with the linker self-association through urea...urea hydrogen bonding. The simple *N,N'*-bis-(*m*-pyridyl)urea (BPU) linker, on the other hand, proved to

- (4) (a) Snurr, R. Q.; Hupp, J. T.; Nguyen, S. T. *AIChE J.* **2004**, *50*, 1090. (b) Suslick, K. S.; Bhyrappa, P.; Chou, J. H.; Kosal, M. E.; Nakagaki, S.; Smithery, D. W.; Wilson, S. R. *Acc. Chem. Res.* **2005**, *38*, 283. (c) Pan, L.; Olson, D. H.; Ciemmolonski, L. R.; Heddy, R.; Li, J. *Angew. Chem., Int. Ed.* **2006**, *45*, 616. (d) Chen, B.; Liang, C.; Yang, J.; Contreras, D. S.; Clancy, Y. L.; Lobkovsky, E. B.; Yaghi, O. M.; Dai, S. *Angew. Chem., Int. Ed.* **2006**, *45*, 1390.
- (5) (a) Yaghi, O. M.; Li, H. *J. Am. Chem. Soc.* **1996**, *118*, 295. (b) Min, K. S.; Suh, M. P. *J. Am. Chem. Soc.* **2000**, *122*, 6834. (c) Lee, E.; Kim, J.; Heo, J.; Whang, D.; Kim, K. *Angew. Chem., Int. Ed.* **2001**, *40*, 399. (d) Noro, S.-I.; Kitaura, R.; Kondo, M.; Kitagawa, S.; Ishii, T.; Matsuzaka, H.; Yamashita, M. *J. Am. Chem. Soc.* **2002**, *124*, 2568. (e) Muthu, S.; Yip, J. H. K.; Vittal, J. J. *J. Chem. Soc., Dalton Trans.* **2002**, 4561. (f) Dalrymple, S. A.; Shimizu, G. K. H. *Chem.—Eur. J.* **2002**, *8*, 3011. (g) Fan, J.; Gan, L.; Kawaguchi, H.; Sun, W.-Y.; Yu, K.-B.; Tang, W.-X. *Chem.—Eur. J.* **2003**, *9*, 3965. (h) Hamilton, B. H.; Kelly, K. A.; Wagler, T. A.; Espe, M. P.; Ziegler, C. J. *Inorg. Chem.* **2004**, *43*, 50.
- (6) Noble, R. D.; Agrawal, R. *Ind. Eng. Chem. Res.* **2005**, *44*, 2887.
- (7) Khlobystov, A. N.; Champness, N. R.; Roberts, C. J.; Tendler, S. J. B.; Thompson, C.; Schröder, M. *CrystEngComm.* **2002**, *4*, 426.
- (8) Custelcean, R.; Gorbunova, M. G. *J. Am. Chem. Soc.* **2005**, *127*, 16362.

- (9) Moyer, B. A.; Bonnesen, P. V. *Physical Factors in Anion Separations in Supramolecular Chemistry of Anions*; Bianchi, A., Bowman-James, K., Garcia-España, E., Eds.; Wiley-VCH: New York, 1997.
- (10) (a) Levitskaia, T. G.; Marquez, M.; Sessler, J. L.; Shriver, J. A.; Vercouter, T.; Moyer, B. A. *Chem. Commun.* **2003**, 2248. (b) Sisson, A. L.; Clare, J. P.; Davis, A. P. *Chem. Commun.* **2005**, 5263.
- (11) (a) Antonisse, M. M. G.; Snellink-Ruel, B. H. M.; Ion, A. C.; Engbersen, J. F. J.; Reinhoudt, D. N. *J. Chem. Soc., Perkin Trans. 2*, **1999**, 1211. (b) Steinle, E. D.; Schaller, U.; Meyerhoff, M. E. *Anal. Sci.* **1998**, *14*, 79.
- (12) (a) Hay, B. P.; Firman, T. K.; Moyer, B. A. *J. Am. Chem. Soc.* **2005**, *127*, 1810 and references therein. (b) Boiocchi, M.; Del Boca, L.; Gomez, D. E.; Fabbri, L.; Licchelli, M.; Monzani, E. *J. Am. Chem. Soc.* **2004**, *126*, 16507.
- (13) Custelcean, R.; Moyer, B. A.; Hay, B. P. *Chem. Commun.* **2005**, 5971.

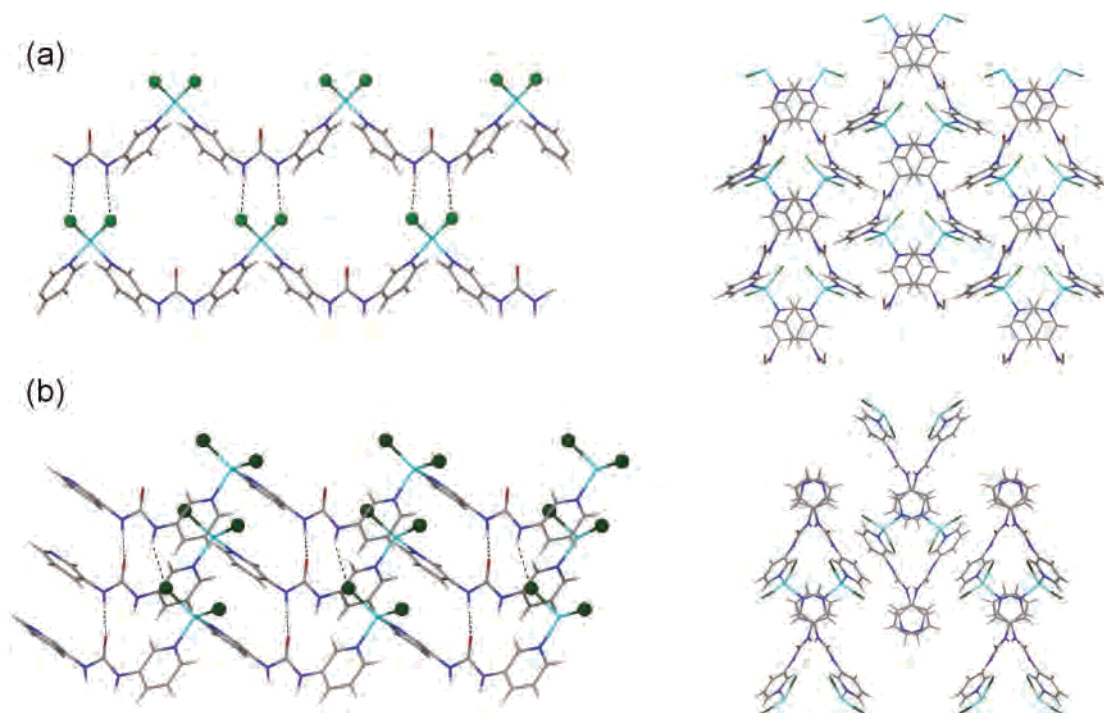


Figure 1. (a) Crystal structure of **1** showing the one-dimensional ZnCl_2 -BPU coordination chains hydrogen-bonded into layers by urea $\cdots\text{Cl}_2\text{Zn}$ hydrogen bonds (left) and the packing of layers (right). (b) Crystal structure of **2** (isostructural with **3**) showing the one-dimensional ZnBr_2 -BPU coordination chains hydrogen-bonded into layers by urea \cdots urea and urea $\cdots\text{Br-Zn}$ hydrogen bonds (left) and the packing of layers (right). Cl and Br are shown as green balls, and the MOFs are shown as stick models.

be a versatile anion binder when incorporated into MOFs due to the enhanced acidity of the urea group and its decreased tendency for self-association.¹⁴ In the present study, we employed this linker for the separation of anions through competitive crystallization of zinc coordination polymers. We demonstrate that the one-dimensional frameworks self-assembled from BPU and Zn^{2+} selectively include halides upon crystallization from aqueous mixtures containing equivalent concentrations of Cl^- , Br^- , I^- , SO_4^{2-} , NO_3^- , and ClO_4^- , with an observed anti-Hofmeister selectivity. This study represents, to our knowledge, the first attempt to separate anions on the basis of their competitive crystallization within MOFs.¹⁵ Moreover, the coordination polymers described here share common structural frameworks, to the extent that concomitant inclusion of various proportions of halides with the formation of solid solutions was observed, which simplifies the interpretation of the observed selectivity on the basis of the coordination environment of the included anions inside the crystals.

Results and Discussion

BPU forms one-dimensional coordination polymers with ZnCl_2 , ZnBr_2 , ZnI_2 , and ZnSO_4 that precipitate from water-ethanol mixtures. On the other hand, $\text{Zn}(\text{ClO}_4)_2$ forms a discrete, soluble coordination complex from the same solvents, while $\text{Zn}(\text{NO}_3)_2$ does not form any coordination solid, and only crystals of $\text{BPU}\cdot(\text{H}_2\text{O})_2$ are isolated under

these conditions.¹⁴ The structure of the MOF obtained from ZnSO_4 has been previously published and consists of octahedral Zn nodes coordinated by two pyridine groups, a monodentate sulfate, and three ancillary water molecules. The resulting one-dimensional chains are further linked by sulfate-urea and sulfate-water hydrogen bonds into a three-dimensional network that entraps one equivalent of ethanol solvent.¹⁴

Figure 1 depicts the crystal structures of $\text{ZnCl}_2(\text{BPU})$ (**1**) and the two isostructural MOFs $\text{ZnBr}_2(\text{BPU})$ (**2**) and $\text{ZnI}_2(\text{BPU})$ (**3**). All three structures consist of tetrahedral Zn nodes coordinated by two halide ions and two pyridine groups, resulting in one-dimensional coordination chains. The chains in **1** are further linked by chelate urea $\cdots\text{Cl}_2\text{Zn}$ hydrogen bonds [$\text{R}^2_2(8)$ graph set notation] into two-dimensional layers, with an observed $\text{H}\cdots\text{Cl}$ distance of 2.51 Å and a $\text{N-H}\cdots\text{Cl}$ angle of 150.2°. Stacking of the layers by van der Waals interactions completes the crystal packing of **1**. Hydrogen bonding between metal-bound chlorides and various proton donors, including urea, are well-documented.¹⁶ Among such structures, the six-member-ring $\text{R}^2_1(6)$ motif involving only one X-M that forms a bifurcated hydrogen bond to urea, however, prevails over the eight-member $\text{R}^2_2(8)$ ring motif observed here. Metal-bound bromide and iodide, on the other hand, are weaker hydrogen-bond acceptors. Accordingly, the coordination chains in **2** and **3** are interlinked in layers by

(14) Custelcean, R.; Moyer, B. A.; Bryantsev, V. S.; Hay, B. P. *Cryst. Growth Des.* **2006**, *6*, 555.

(15) For a recent example of pairwise competitive crystallization of anions based on metal coordination in discrete complexes, see: Chen, X.-D.; Mak, T. C. W. *Chem. Commun.* **2005**, 3529.

(16) (a) Aullón, G.; Bellamy, D.; Brammer, L.; Bruton, E. A.; Orpen, A. G. *Chem. Commun.* **1998**, 653. (b) Brammer, L.; Bruton, E. A.; Sherwood, P. *Cryst. Growth Des.* **2001**, *1*, 277. (c) Turner, D. R.; Smith, B.; Goeta, A. E.; Radosavljevic Evans, I.; Tocher, D. A.; Howard, J. A. K.; Steed, J. W. *CrystEngComm.* **2004**, *6*, 633. (d) Kumar, D. K.; Das, A.; Dastidar, P. *Cryst. Growth Des.* **2005**, *5*, 651.

urea...urea hydrogen bonds instead,¹⁷ via one of the NH protons, with H...O contact distances of 2.13 and 2.31 Å and N–H...O angles of 152.5° and 148.6°, respectively. The second NH proton interacts with a Br[−] or I[−] from a second-neighbor chain, with observed H...X distances of 2.64 and 2.80 Å and N–H...X angles of 149.5° and 149.6°, respectively. Finally, the layers pack along the remaining direction by van der Waals interactions.

The FTIR spectrum of **1** displays characteristic peaks for the urea group: 3302 and 1706 cm^{−1}, corresponding to the N–H and C=O stretching modes, respectively. For comparison, **2** and **3** display two N–H stretching modes, one at 3348 and 3342 cm^{−1}, respectively, corresponding to the NH group hydrogen-bonded to the halide, and another one at 3251 and 3310 cm^{−1}, respectively, corresponding to the NH group hydrogen-bonded to urea. Also, the C=O stretching modes observed in **2** (1672 cm^{−1}) and **3** (1681 cm^{−1}) are red-shifted relative to **1** as a result of urea...urea hydrogen bonding.

Crystallization of a 1:1 mixture of ZnCl₂ and ZnBr₂ with a stoichiometric amount of BPU from water–ethanol resulted, after 1 month, in the concomitant formation of two different crystalline phases, which were analyzed by single-crystal X-ray diffraction. The first phase (**4**), representing the large majority of the crystallized solid, was found to be isostructural with ZnBr₂(BPU), with Br[−] and Cl[−], however, sharing the same sites in the framework, thus generating a mixed crystal. As depicted in Figure 1b, there are two nonequivalent Br[−] sites in **2**, with one hydrogen-bonded to urea and the other one not. The hydrogen-bonded site in **4** contains 66% Cl[−], while the non-hydrogen-bonded site contains only 40% Cl[−], with the Br[−] occupying the remaining 34% and 60% of the two sites, respectively [corresponding to the ZnCl_{1.06}Br_{0.94}(BPU) overall composition for **4**]. As a consequence of the partial substitution with Cl, the NH...Br(Cl) and NH...O hydrogen bonds in **4** are shortened by 0.14 and 0.04 Å, respectively, relative to **2**. In addition to the major phase **4**, a few crystals of a different phase (**5**) were isolated from the same crystallization batch. Single-crystal X-ray diffraction revealed that this phase is isostructural with ZnCl₂(BPU) and, like **4**, is a solid solution containing both Cl[−] and Br[−]. The two equivalent hydrogen-bonded halide sites in this phase (Figure 1a) are occupied by 71% Cl[−] and 29% Br[−], which corresponds to the composition ZnCl_{1.42}Br_{0.58}(BPU) for **5**. The NH...Cl(Br) hydrogen-bonding distance in **5** is consequently elongated by 0.05 Å relative to **1** as a result of the partial substitution of Cl[−] with Br[−].

In a similar experiment, the crystallization of a 1:1 mixture of ZnBr₂ and ZnI₂ with two equivalents of BPU generated after 1 month another mixed crystalline phase (**6**), isostructural with **2** and **3**, and with geometrical parameters intermediate between those found in the two pure phases. The Br[−] and I[−] share the same sites in the crystal, though in

different proportions depending on the particular site. Thus, the urea-bonded site contains 59% Br[−], whereas the non-hydrogen-bonded site contains only 33% Br[−], with the I[−] occupying the remaining 41% and 67% of the two sites, respectively, which corresponds to the overall crystal composition of ZnBr_{0.92}I_{1.08}(BPU). The NH...Br(I) and NH...O hydrogen-bond contacts in **6**, of 2.68 and 2.19 Å, are intermediate between the corresponding distances in **2** and **3**. An even more pronounced segregation of halides was observed by structural analysis in a mixed crystal obtained from a 1:1 mixture of ZnCl₂ and ZnI₂ (**7**), which had a composition of ZnCl_{1.11}I_{0.89}(BPU) and was isostructural with **2** and **3**. The hydrogen-bonded halide site in this crystal contains 85% Cl[−], while the non-hydrogen-bonded site contains only 26% Cl[−], with I[−] occupying the remaining 15% and 74% of the two sites, respectively. The NH...Cl(I) and NH...O hydrogen-bond contacts in **7**, of 2.49 and 2.08 Å, are considerably shorter than the analogous distances in **3**, as a result of partial substitution with chloride.

The concomitant inclusion of various halides in the mixed crystals **4**–**7** allows the evaluation of the halide selectivity of different sites in these crystals as a function of their immediate coordination environments. Thus, in **5**, all sites are equivalent and offer a strong coordination environment for the halides, consisting of strong interactions with the Zn²⁺ centers and urea hydrogen-bonding groups (Figure 1a). This “acidic” environment favors the more densely charged Cl[−], against the less hydrophilic Br[−]. In **4**, **6**, and **7**, on the other hand, there are two different coordination sites for the halides. While overall the halides are included in roughly the same proportions in these crystals, there is significant site selectivity as shown by the X-ray structural analysis, with the more acidic site hydrogen-bonded to urea including significantly more of the more-basic halide. The less basic, less hydrophilic halide prefers the non-hydrogen-bonded site, where the van der Waals interactions, favoring larger, more polarizable anions, predominate.

The total exclusion of nitrate and perchlorate and the observed partial discrimination among halides by the Zn–BPU MOFs, as indicated by the single-crystal X-ray diffraction experiments, suggested to us the possibility for anion separation with this coordination framework through competitive crystallization. To test this idea, 0.1 mmol of BPU dissolved into 3 mL of ethanol was added over an aqueous solution (4 mL) containing 0.1 mmol of Zn(NO₃)₂; 0.2 mmol of each NaCl, NaBr, NaI, NaClO₄; and 0.1 mmol of Na₂SO₄. The amounts of Zn²⁺ and BPU were thereby limited so that only a total amount of 0.1 mmol of Zn–BPU MOF could be theoretically formed, which, however, might contain various fractions of the competing anions depending on their relative affinity to the coordination network. After 30 min, the precipitated solid (**A**) was washed with water and ethanol and was subsequently analyzed by FTIR and elemental analysis to evaluate its anionic composition. As expected, no detectable amounts of NO₃[−] or ClO₄[−] were found in the crystallized material (by FTIR), as these anions do not form MOFs under these conditions. Moreover, the strong peak at 1115 cm^{−1}, corresponding to the sulfate anion in ZnSO₄–

(17) (a) Etter, M. C.; Urbanczyk-Lipkowska, Z.; Zia-Ebrahimi, M.; Panuto, T. W. *J. Am. Chem. Soc.* **1990**, *112*, 8415. (b) Chang, Y. L.; West, M. A.; Fowler, F. W.; Lauher, J. W. *J. Am. Chem. Soc.* **1993**, *115*, 5991.

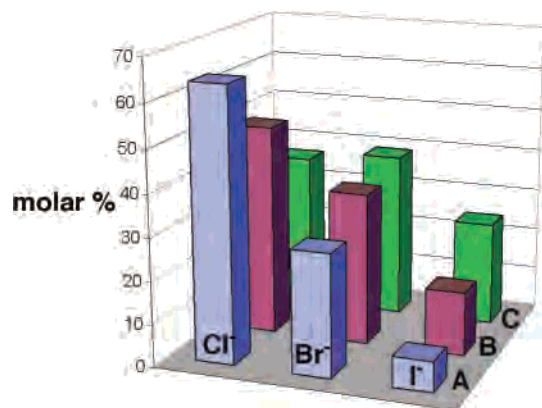


Figure 2. Halide composition of the solids obtained in the competitive crystallization of the Zn–BPU MOFs after 30 min (A), 5 days (B), and 2 weeks (C).

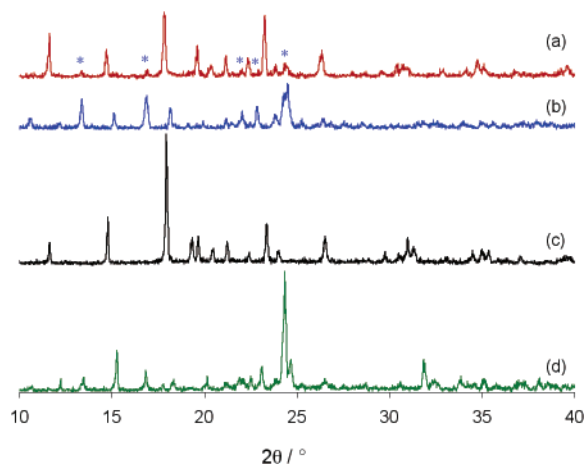


Figure 3. Powder X-ray diffraction patterns of (a) solid **A** consisting of a mixture of structures **1** and **2** (marked by asterisks), (b) solid **B** (isostructural with **C**), (c) **1**, and (d) **2**.

BPU, was completely absent in the FTIR spectrum of **A**, also indicating negligible amounts of this anion. The urea N–H and C=O stretching modes appear at 3308 and 1705 cm^{-1} , which are very close to the values found in **1**, indicating that Cl^- is the major anion present in **A**. The broad and asymmetric shape of these peaks, however, also suggested the presence of Br^- and I^- as minor components. The elemental analysis indeed confirmed that Cl^- , Br^- , and I^- are all present in **A**, with molar ratios of 9.1:4.1:1 (Figure 2). Powder X-ray diffraction analysis showed that **A** is mostly in the ZnCl_2 –BPU form, with a minor amount of the ZnBr_2 –BPU structure present (Figure 3a). The ZnCl_2 –BPU framework, however, is metastable under these conditions and slowly recrystallizes into the ZnBr_2 –BPU structure. Thus, powder X-ray diffraction of the solid isolated after 5 days (**B**) showed the sole presence of the ZnBr_2 –BPU structure (Figure 3b), which was corroborated by FTIR spectroscopy showing the disappearance of the urea modes at 3302 and 1706 cm^{-1} characteristic of the ZnCl_2 –BPU phase. Instead, the observed N–H (3346 and 3237 cm^{-1}) and C=O (1669 cm^{-1}) stretching modes best match the corresponding peaks in **2**. Elemental analysis showed that **B** is a solid solution containing a mixture of all three halides with $\text{Cl}^-/\text{Br}^-/\text{I}^-$ molar ratios of 3.3:2.4:1 (Figure 2). The relative halide

content continues to change if the precipitated solid is left for an even longer time in the supernatant solution, with the $\text{Cl}^-/\text{Br}^-/\text{I}^-$ molar ratios reaching the values of 1.5:1.6:1 after two weeks (solid **C**), as determined by elemental analysis. The powder X-ray pattern of **C**, however, was found virtually unchanged relative to that of **B**. The same elemental and crystallographic composition as found in solid **C** was reached by starting from a suspension of pure ZnCl_2 –BPU crystals in a solution with the content adjusted so that the mixture was isocompositional with those in the previous experiments (experiment **D**), thus confirming the metastable nature of the ZnCl_2 –BPU framework and its recrystallization into the more stable ZnBr_2 –BPU structure under thermodynamic equilibration. These results can be rationalized in terms of packing coefficients¹⁸ of **1** (67.4%) and **2** (72.1%), indicating a more efficient packing, and thus higher stability for the latter, which is corroborated by the higher water solubility measured for **1** (10.1 mmol/L) compared to that of **2** (5.5 mmol/L). The lower discrimination among halides found in the solids **B** and **C** can be rationalized by the reduction in the number of the more selective hydrogen-bonded halide sites compared to **A**, which led to reduced overall selectivity.

Although sulfate has a relatively high charge density and it can form a MOF under the conditions employed here, it proved noncompetitive against the halides for the coordination sites in Zn–BPU, as no measurable amounts of this anion could be detected in our competition experiments. The total exclusion of sulfate from structures **1** and **2** can be rationalized by its considerably larger size compared to the halides, which prevented its inclusion inside these crystals. On the other hand, the $[\text{Zn}(\text{SO}_4)(\text{BPU})(\text{H}_2\text{O})_3](\text{EtOH})$ phase that would normally crystallize in the absence of competing anions¹⁴ was also not observed in the competition experiments, which could be attributed to its slightly higher solubility of 5.7 mmol/L or to kinetic factors.¹⁹

Conclusions

We demonstrated here a new approach for the separation of anions from water by their selective crystallization within MOFs functionalized with urea hydrogen-bonding groups. The most significant results of this study are that Cl^- , Br^- , and I^- were exclusively crystallized against the ClO_4^- , NO_3^- , and SO_4^{2-} oxoanions and that the observed selectivity is opposite of the Hofmeister series typically governing the extraction of anions from water, whether by solvent extraction, anion-exchange with polymeric resins, or coordination polymers. Table 1 summarizes the anion separation selectivities obtained in this study.

The crystallized MOFs adopt common structural frameworks comprising one-dimensional Zn–BPU coordination chains further linked by $\text{NH}\cdots\text{X}$ ($\text{X} = \text{Cl}^-$, Br^- , and I^-) or $\text{urea}\cdots\text{urea}$ hydrogen bonding, thus allowing the concomitant

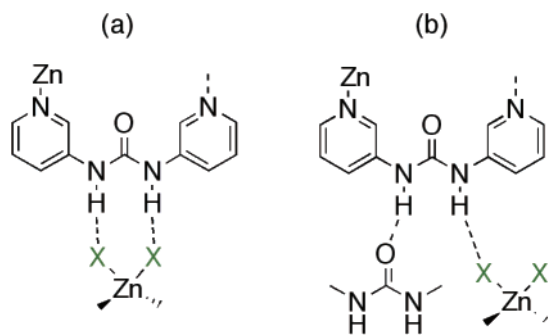
(18) Sluis, P. v. d.; Spek, A. L. *Acta Crystallogr., Sect. A* **1990**, *46*, 194.

(19) The total concentration of halides is 6 times larger than the concentration of sulfate in the competition experiments. Furthermore, the inclusion of ethanol and water inside the sulfate framework is also expected to result in unfavorable entropy and a lower nucleation rate for the formation of this crystal.

Table 1. Anion Separation Selectivities Expressed as Separation Factors $\alpha(X/Y) = [(\text{mol } X)/(\text{mol } Y)]_{\text{precipitated solid}} / [(\text{mol } X)/(\text{mol } Y)]_{\text{supernatant solution}}$

separation factor	expt A	expt B	expt C
$\alpha(\text{Cl}/\text{Br})$	2.84	1.64	0.92
$\alpha(\text{Cl}/\text{I})$	13.37	4.75	1.64
$\alpha(\text{Cl}/\text{SO}_4)$	∞	∞	∞
$\alpha(\text{Cl}/\text{NO}_3)$	∞	∞	∞
$\alpha(\text{Cl}/\text{ClO}_4)$	∞	∞	∞

Chart 1



inclusion of all three halides in the same structures with the formation of solid solutions. This rare circumstance offered a unique opportunity for the unambiguous interpretation of the observed halide selectivities on the basis of the coordination environment of the halides within the frameworks, which facilitated the formulation of structure-selectivity principles in this series of coordination polymers. Crystallization under kinetic control enabled a more selective halide separation through initial precipitation of the metastable ZnCl_2 -BPU phase, with the Zn^{2+} Lewis acid centers and urea hydrogen-bonding groups acting concurrently as binding sites for the included halides (Chart 1a). Under these conditions, the smaller, more densely charged chloride is preferred against the larger, less hydrophilic Br^- or I^- . Under thermodynamic equilibration, however, the ZnCl_2 -BPU phase redissolved and the more stable ZnBr_2 -BPU phase precipitated as a solid solution including a mixture of the three halides. Crystal structure analysis revealed two different halide sites in this phase, with only one of them displaying the more selective hydrogen-bonding interactions to urea, which translated into lower discrimination among halides (Chart 1b).

Thus, within each of the two structural frameworks observed, the anion inclusion selectivity appears to be governed, on one hand, by the anion size, which resulted in exclusion of the larger oxoanions, and, on the other hand, by the anion basicity and its coordinating ability, which resulted in discrimination among halides. While these factors have long been known to influence anion binding by synthetic receptors in solution, this study demonstrated that the same principles may be transferred to crystalline coordination networks, with the caveat that, with the latter, the solubility of the crystallized framework, which ultimately depends on its overall crystal packing efficiency, may also play a decisive role in the observed anion-separation selectivity. Accordingly, in addition to the rigorous design of the anion-binding cavity, a judicious approach toward novel crystalline materials with advanced anion extraction properties will require precise control of their three-

dimensional crystal architecture. We anticipate that the design of more elaborate linkers with multiple complementary hydrogen-bonding groups capable of shape recognition of more complex anions, and their incorporation into networks sharing a common, persistent structural framework, will ultimately lead to a more rational and general approach toward anion separations with MOFs.

Experimental Section

Reagents and solvents were purchased from commercial suppliers and used without further purification. BPU was prepared as previously described.¹⁴ Powder X-ray diffraction patterns were obtained with a Bruker D5005 diffractometer using monochromatic $\text{Cu K}\alpha$ radiation ($\lambda = 1.5418 \text{ \AA}$). FTIR spectra were recorded in KBr pellets with a Digilab FTS 7000 spectrometer. MOF solubilities in water were measured by Zn^{2+} analysis of saturated solutions (diluted 20-fold) with a Thermo-Electron model IRIS Intrepid II XSP dual view inductively coupled argon plasma optical emission spectrometer. The wavelength at 213.8 nm was analyzed using the radial torch orientation for concentrations falling on a standard curve from 1 to 100 ppm. Elemental analyses were performed by Desert Analytics, Tucson, Arizona.

Safety Note. Perchlorate salts of metal complexes with organic ligands are potentially explosive. Although no problem was encountered in the present study, care must be exercised when handling such compounds.

$\text{ZnCl}_2(\text{BPU})$ (1). A solution of BPU (0.043 g, 0.2 mmol) in 3 mL of EtOH was layered over a solution of ZnCl_2 (0.014 g, 0.1 mmol) in 2 mL of deionized water. Colorless crystals of **1** were collected after 4 days and washed with EtOH. Yield: quantitative. FTIR (KBr): ν 3302 s, 3073 w, 1706 m, 1613 w, 1588 m, 1530 m, 1478 w, 1425 s, 1333 m, 1267 m, 1216 m, 1109 w, 1060 w, 914 w, 822 w, 785 w, 743 w, 697 w, 652 w, 585 w. Anal. Calcd for $\text{C}_{11}\text{H}_{10}\text{N}_4\text{Cl}_2\text{OZn}$: C, 37.69; H, 2.88; N, 15.98. Found: C, 37.74; H, 2.84; N, 15.83.

$\text{ZnBr}_2(\text{BPU})$ (2). A solution of BPU (0.043 g, 0.2 mmol) in 3 mL of EtOH was layered over a solution of ZnBr_2 (0.023 g, 0.1 mmol) in 2 mL of deionized water. Colorless crystals of **2** were collected after 4 days and washed with EtOH. Yield: 0.020 g (46%). FTIR (KBr): ν 3348 m, 3251 m, 3072 w, 1672 s, 1613 m, 1587 s, 1540 s, 1474 m, 1429 s, 1333 m, 1267 s, 1223 s, 1128 w, 1102 w, 1056 w, 911 w, 800 w, 781 m, 733 m, 692 m, 650 m, 543 w, 509 w. Anal. Calcd for $\text{C}_{11}\text{H}_{10}\text{N}_4\text{Br}_2\text{OZn}$: C, 30.07; H, 2.29; N, 12.75. Found: C, 30.32; H, 2.42; N, 12.61.

$\text{ZnI}_2(\text{BPU})$ (3). A solution of BPU (0.043 g, 0.2 mmol) in 3 mL of EtOH was layered over a solution of ZnI_2 (0.032 g, 0.1 mmol) in 2 mL of deionized water. Colorless crystals of **3** were collected after 4 days and washed with EtOH. Yield: 0.027 g (51%). FTIR (KBr): ν 3342 m, 3310 sh, 3070 w, 1681 s, 1611 w, 1584 s, 1539 s, 1502 w, 1474 w, 1430 s, 1331 w, 1291 w, 1264 s, 1216 m, 1126 w, 1102 w, 1055 w, 801 w, 781 w, 722 w, 691 m, 648 w, 513 m. Anal. Calcd for $\text{C}_{11}\text{H}_{10}\text{N}_4\text{I}_2\text{OZn}$: C, 24.77; H, 1.89; N, 10.50. Found: C, 25.08; H, 2.14; N, 10.32.

Competitive Crystallization Experiments. A solution of BPU (0.021 g, 0.1 mmol) in 3 mL of EtOH was added over a solution containing NaCl (0.012 g, 0.2 mmol), NaBr (0.020 g, 0.2 mmol), NaI (0.030 g, 0.2 mmol), NaClO_4 (0.024 g, 0.2 mmol), Na_2SO_4 (0.014 g, 0.1 mmol), and $\text{Zn}(\text{NO}_3)_2 \cdot 4\text{H}_2\text{O}$ (0.026 g, 0.1 mmol) in 4 mL of deionized water, and the resulting mixture was left undisturbed at room temperature. The precipitated solid was filtered after 30 min (expt A), 5 days (expt B), or 2 weeks (expt C) and

Table 2. Crystallographic Data for **1–3**

	1	2	3
formula	C ₁₁ H ₁₀ Cl ₂ N ₄ OZn	C ₁₁ H ₁₀ Br ₂ N ₄ OZn	C ₁₁ H ₁₀ I ₂ N ₄ OZn
mol wt	350.50	439.42	533.40
cryst size [mm]	0.49 × 0.20 × 0.19	0.36 × 0.30 × 0.16	0.44 × 0.24 × 0.19
cryst syst	orthorhombic	monoclinic	monoclinic
space group	<i>Fdd2</i>	<i>P2₁/c</i>	<i>P2₁/c</i>
<i>a</i> [Å]	18.230(2)	10.0599(11)	10.1499(11)
<i>b</i> [Å]	9.8294(11)	16.7628(18)	17.1161(19)
<i>c</i> [Å]	15.8794(17)	8.4195(9)	8.7576(10)
α [deg]	90	90	90
β [deg]	90	103.996(2)	104.884(2)
γ [deg]	90	90	90
<i>V</i> [Å ³]	2845.4(5)	1377.6(3)	1470.4(3)
<i>Z</i>	8	4	4
<i>T</i> [K]	173(2)	173(2)	173(2)
ρ _{calcd} [g cm ⁻³]	1.636	2.119	2.410
2θ _{max} [deg]	56.70	56.64	56.62
μ [cm ⁻¹]	2.097	7.579	5.866
reflns collected	7762	17 145	17 677
independent reflns	1780	3432	3661
params	89	172	172
<i>R</i> ₁ , ^a w <i>R</i> ₂ ^b [<i>I</i> > 2σ(<i>I</i>)]	0.0152, 0.0395	0.0190, 0.0495	0.0195, 0.0478
GOF	1.050	1.047	1.202

$${}^a R_1 = \sum(|F_o| - |F_c|)/\sum|F_o|. \quad {}^b wR_2 = \{\sum[w(F_o^2 - F_c^2)^2]/\sum[w(F_o^2)]\}^{1/2}.$$

Table 3. Crystallographic Data for the Mixed Crystals **4–7**

	4	5	6	7
formula	C ₁₁ H ₁₀ Cl _{1.06} Br _{0.94} N ₄ OZn	C ₁₁ H ₁₀ Cl _{1.42} Br _{0.58} N ₄ OZn	C ₁₁ H ₁₀ Br _{0.92} I _{1.08} N ₄ OZn	C ₁₁ H ₁₀ Cl _{1.11} I _{0.89} N ₄ OZn
mol wt	392.29	376.29	490.17	431.89
cryst size [mm]	0.25 × 0.13 × 0.10	0.35 × 0.21 × 0.17	0.23 × 0.12 × 0.11	0.14 × 0.05 × 0.04
cryst syst	monoclinic	orthorhombic	monoclinic	monoclinic
space group	<i>P2₁/c</i>	<i>Fdd2</i>	<i>P2₁/c</i>	<i>P2₁/c</i>
<i>a</i> [Å]	10.0302(16)	18.3673(12)	10.0935(9)	9.9971(9)
<i>b</i> [Å]	16.7652(19)	9.8780(6)	17.0287(16)	17.3712(7)
<i>c</i> [Å]	8.3591(11)	15.9371(10)	8.5845(8)	8.5845(8)
α [deg]	90	90	90	90
β [deg]	105.098(16)	90	104.658(2)	105.256(2)
γ [deg]	90	90	90	90
<i>V</i> [Å ³]	1357.1(3)	2891.5(3)	1427.5(2)	1387.6(2)
<i>Z</i>	4	8	4	4
<i>T</i> [K]	173(2)	173(2)	173(2)	173(2)
ρ _{calcd} [g cm ⁻³]	1.920	1.729	2.281	2.067
2θ _{max} [deg]	56.60	56.58	56.66	56.66
μ [cm ⁻¹]	4.781	3.560	6.628	3.960
reflns collected	8020	4269	12474	13926
independent reflns	3244	1674	3560	3454
params	174	90	174	174
<i>R</i> ₁ , ^a w <i>R</i> ₂ ^b [<i>I</i> > 2σ(<i>I</i>)]	0.0266, 0.0653	0.0155 0.0397	0.0278, 0.0571	0.0449, 0.1142
GOF	1.098	1.044	1.282	1.129

$${}^a R_1 = \sum(|F_o| - |F_c|)/\sum|F_o|. \quad {}^b wR_2 = \{\sum[w(F_o^2 - F_c^2)^2]/\sum[w(F_o^2)]\}^{1/2}.$$

washed with water and EtOH. Yield: 0.021 g, 54% (**A**); 0.032 g, 78% (**B**); 0.028 g, 65% (**C**).

Experiment D. A polycrystalline fine powder of **1** (0.0175 g, 0.05 mmol) was suspended in a solution of NaCl (0.006 g, 0.1 mmol), NaBr (0.020 g, 0.2 mmol), NaI (0.030 g, 0.2 mmol), NaClO₄ (0.024 g, 0.2 mmol), Na₂SO₄ (0.014 g, 0.1 mmol), and Zn(NO₃)₂·4H₂O (0.013 g, 0.05 mmol) in 4 mL of deionized water and BPU (0.011 g, 0.05 mmol) in 3 mL of EtOH. The mixture was left undisturbed at room temperature for 5 days, and the precipitate was filtered and washed with water/ethanol. Yield: 0.032 g, 74%.

X-ray Crystallography. Single-crystal X-ray data were collected on a Bruker SMART APEX CCD diffractometer with fine-focus Mo Kα radiation (λ = 0.710 73 Å), operated at 50 kV and 30 mA. All structures were solved by direct methods and refined on *F*² using the SHELXTL software package.²⁰ Absorption corrections

were applied using SADABS, part of the SHELXTL package. All non-hydrogen atoms were refined anisotropically. Hydrogen atoms were placed in idealized positions and refined with a riding model. Pertinent crystallographic data for **1–7** are listed in Tables 2 and 3 and in the Supporting Information.

Acknowledgment. This research was sponsored by the Division of Chemical Sciences, Geosciences, and Biosciences, Office of Basic Energy Sciences, U.S. Department of Energy, under contract number DE-AC05-00OR22725 with Oak Ridge National Laboratory managed by U. T.—Battelle, LLC.

Supporting Information Available: Crystallographic data in CIF format and figures of structures **1–7** as thermal ellipsoids plots. This material is available free of charge via the Internet at <http://pubs.acs.org>.

(20) SHELXTL, version 6.12; Bruker AXS, Inc.: Madison, WI, 1997.